Published in final edited form as:
Toxicol Appl Pharmacol. 2012 December 1; 265(2): . doi:10.1016/j.taap.2012.10.008.

Gene expression profiling and pathway analysis of human bronchial epithelial cells exposed to airborne particulate matter collected from Saudi Arabia

Hong Sun[1], **Magdy Shamy**[2], **Thomas Kluz**[1], **Alexandra B. Muñoz**[1], **Mianhua Zhong**[1], **Freda Laulicht**[1], **Mansour A. Alghamdi**[2], **Mamdouh I. Khoder**[2], **Lung-Chi Chen**[1], and **Max Costa**[1,*]

[1]Department of Environmental Medicine, NYU School of Medicine, Tuxedo, NY, USA

[2]Department of Environmental Sciences, Faculty of Meteorology, Environment and Arid Land Agriculture, King Abdulaziz University, Jeddah, Saudi Arabia

Abstract

Epidemiological studies have established a positive correlation between human mortality and increased concentration of airborne particulate matters (PM). However, the mechanisms underlying PM related human diseases, as well as the molecules and pathways mediating the cellular response to PM, are not fully understood. This study aims to investigate the global gene expression changes in human cells exposed to PM_{10} and to identify genes and pathways that may contribute to PM related adverse health effects. Human bronchial epithelial cells were exposed to PM_{10} collected from Saudi Arabia for 1 or 4 days, and whole transcript expression was profiled using the GeneChip human gene 1.0 ST array. A total of 140 and 230 genes were identified that significantly changed more than 1.5 fold after PM_{10} exposure for 1 or 4 days, respectively. Ingenuity Pathway Analysis revealed that different exposure durations triggered distinct pathways. Genes involved in NRF2-mediated response to oxidative stress were up-regulated after 1 day exposure. In contrast, cells exposed for 4 days exhibited significant changes in genes related to cholesterol and lipid synthesis pathways. These observed changes in cellular oxidative stress and lipid synthesis might contribute to PM related respiratory and cardiovascular disease.

Keywords

particulate matter; gene expression; human bronchial epithelial cells; Microarray; Ingenuity pathway analysis

Introduction

Airborne particulate matter, comprised of a mixture of dust, dirt, smoke, and liquid droplets, has been linked to many adverse health effects including respiratory and cardiovascular problems. Numerous epidemiological studies have established an association between short- or long-term exposure to various airborne particulates and human mortality and morbidity (Rückerl et al. 2011; Schwarze et al. 2006; Chen and Lippmann 2009). Studies have found a significant correlation between excess mortality and short-term exposure to high concentration of ambient particulate matters (Bell and Davis 2001; Schwartz and Marcus 1990). Also, a population-based study on data collected in 6 US cities suggested an association between long-term exposure and human mortality (Dockery et al. 1993; Laden et

*Corresponding author. Mailing Address: Department of Environmental Medicine, NYU School of Medicine, 57 Old Forge Road, Tuxedo, New York 10987, Phone: (845) 731-3515, Fax: (845) 351-2118, Max.Costa@nyumc.org.

al. 2000). In addition to mortality, airborne particulates were found to connect to increased morbidity. A number of studies reported an association between respiratory and cardiovascular symptoms and short- or long-term exposure to high level of ambient particles (Pope 1989; Brook et al. 2010; Zanobetti and Schwartz 2007). As a result, the mechanisms underlying the PM induced adverse health effects have become an area of active research.

Both *in vitro* and *in vivo* studies have established the role of reactive oxygen species (ROS) in PM-induced respiratory and cardiovascular diseases (Ghio et al. 2012; Araujo and Nel 2009; Møller et al. 2010). Following PM exposure, ROS can be generated by some PM components, such as transition metals and organics (Cho et al. 2005; Becker et al. 2005). High level of ROS production could lead to cell apoptosis and tissue damage, which may contribute to lung injury as seen in human or animal models following acute exposure to PM. In addition, ROS are able to initiate a series of redox signaling cascades to induce inflammatory responses and cytokine production found in both acute and chronic PM exposures (Akhtar et al. 2010; Diabaté et al. 2011).

Although PM exposure causes adverse health effects, the magnitude of these effects depends on many factors: particle size, source, chemical composition, and exposure duration, etc (Araujo and Nel 2009; Gordon 2007). While coarse PM (aerodynamic size between 2.5 and 10 μm) can deposit in the upper respiratory tract and lung, fine (≤2.5 μm) and ultrafine (≤0.1 μm) PM penetrate deeper into the alveolar region of the lung resulting in more profound effects on the cardiovascular system. The major sources of PM include soil, dust, crustal particles, fuel combustion, oil refinery and metal processing facilities, and are normally linked to many geographical and meteorological variables (Simkhovich et al. 2008; Araujo and Nel 2009). The chemical composition, which varies depending on the source, is a major factor that contributes to the adverse health effects of PM. Several *in vitro* and *in vivo* studies reported the effects of metals, in particular transition metals, on PM induced inflammatory response and cytotoxic activities (Chen and Lippmann 2009).

In the Middle East, dust and sand storm are important factors contributing to airborne particulates. Chronic inhalation of sand dust has been shown to lead to the development of Desert Lung Syndrome, a rare non-progressive non-occupational lung disease found in desert inhabitants (Waness et al. 2011; Nouh 1989). Silicosis and asthma are also linked to desert sand exposure. In the past decade, with the rapid industrialization and increased oil combustion, air pollution has become a serious problem. When combined with sand dust, air pollution likely contributes to significant increases in public health problems, such as cardiovascular and respiratory disease, cancer, and diabetes mellitus. In 2010, the top three causes of death in Saudi Arabia were coronary heart disease (CHD, 24%), hypertension (12%) and diabetes mellitus (6.7%) (http://www.worldlifeexpectancy.com/country-health-profile/saudi-arabia).

Recently, we have conducted a multi-week, multiple site sampling campaign to study the source apportionment and elemental composition of PM_{10} and $PM_{2.5}$ in Jeddah, the second largest city in Saudi Arabia. The results showed that the major source factors for PM_{10} or $PM_{2.5}$ were soil resuspension, oil combustion, mixed industrial sources, traffic sources, and marine aerosols (manuscript submitted). To investigate the impact of PM exposure on human bronchial cells, we analyzed global gene expression profiles following exposure of cells to PM_{10}. Given that lungs are the major organs targeted by the various sized PM particles, human bronchial epithelial BEAS-2B cells were chosen to expose to the PM_{10} samples (including coarse, fine and ultrafine PM) for either a short-term (1 day) or longer-term (4 days) duration. Differentially expressed genes following PM_{10} exposure were identified and analyzed for networks and pathways that may contribute to the cellular response to PM.

Materials and Methods

Particle sample collection

Dust samples were collected from the campus of King Abdulaziz University located in south Jeddah. For metal composition analysis, PM_{10} (≤10 μm) was collected for 24 hours through Automated Cartridge Collector Unit (ACCU) sampler onto pre-weighed Teflon (GelmanTeflo, 37mm, 0.2 um pore). For *in vitro* exposure, particles were collected for 48 hours on 5300 Polypropylene filters using Staplex high volume air sampler (Staplex Air Sampler Division, USA) with PM_{10} inlet (serial NO. 2840) at a fixed flow rate of 900 l/min.

Element metal analysis

Metal concentration was analyzed as follows: The mass on the Teflon filter was measured using a microbalance (model MT5, Mettler-Toledo Inc.) in a temperature and humidity controlled weighing room at NYU laboratory. The concentration of metals was analyzed using a nondestructive X-ray Fluorescence (XRF) Spectrometer (EX-6600-AF, Jordan Valley) with five secondary fluorescers (Si, Ti, Fe, Ge, and Mo) and spectral software XRF2000v3.1 (U.S. EPA and ManTech Environmental Technology, Inc.) as described previously (Maciejczyk and Chen 2005).

Particle extraction

PM_{10} particles were extracted from polypropylene filters using a modified aqueous extraction protocol (Duvall et al. 2008). Briefly, each filter was wetted with 25 ml of 70% ethanol followed by sonication in 100 ml of distilled water for 2 hours. The particles were dried by lyophilization, then weighed and resuspended in the sterile distilled water, and stored at −80°C.

Cell culture and particle exposure

Normal human bronchial epithelial BEAS-2B cells were cultured in DMEM (Invitrogen) supplemented with 10% FBS and 100 U/ml penicillin and 100 mg/ml streptomycin (Invitrogen). For particle exposure, cells were seeded one day prior to exposure. A small aliquot of particle suspension was mixed with culture medium by sonication for 20 minutes, and then applied evenly to the cultured cells. Untreated and particle treated cells were cultured in 37°C incubator with 5% CO_2 until harvesting at the indicated time intervals.

Colony survival assay

BEAS-2B cells were treated with various concentrations of particles (0, 10, 25, 50, 100, and 200 $\mu g/cm^2$) for 1, 2, 7, and 14 days. Control and particle treated cells were plated at 300 cells/dish in 100-mm cell culture dishes, and cultured for two weeks. Cell colonies were stained with Giemsa solution, and the number of colonies was counted.

RNA extraction and microarray hybridization

BEAS-2B cells were treated with particles (50 $\mu g/cm^2$) that were collected either during normal or storm weather conditions for 1- or 4- days. Total RNA was extracted from control and particle treated cells using Trizol (Invitrogen) and further purified using RNeasy Plus Micro Kit (Qiagen). 100 ng of total RNA was used to synthesize double-stranded cDNA (dsDNA). cRNA was synthesized from dsDNA template, and subsequently used to produce sense single-stranded cDNA (ssDNA) with incorporated deoxyuridine triphosphate. The ssDNAs were fragmented, end-labeled, and hybridized to Affymetrix Human Gene 1.0 ST Array (Affymetrix). Hybridization and scanning of the arrays was performed using a standard procedure.

Microarray data analysis

Microarray data analysis was performed using GeneSpring v12.0 (Agilent Technologies). All microarray data is MIAME compliant and the raw data has been deposited in NCBIs Gene Expression Omnibus (GEO ID: GSE38172). The expression value of each probe set was determined after quantile normalization using RMA algorithm and baseline transformation to the median levels of control samples. Differentially expressed genes were identified using one-way ANOVA ($p<0.05$). Principal component analysis (PCA) was used to visualize the gene expression pattern of all samples. Hierarchical cluster analysis using Euclidean distance was performed to cluster genes and samples to generate a heat map. Functional annotation was analyzed with the Gene Ontology (GO) classification system using DAVID software (http://david.abcc.ncifcrf.gov/home.jsp). Gene network and pathway analysis was performed using Ingenuity Pathway Analysis (http://www.ingenuity.com).

Real time PCR

Total RNA extracted from control and treated cells was converted to single stranded cDNA using Superscrip® III (Invitrogen). Quantitative real-time PCR analysis was performed using SYBR green PCR system (Applied Biosystems) on ABI prism 7900HT system (Applied Biosystems). Relative gene expression levels were normalized to ACTB expression. All PCR reactions were performed in triplicate. Results were presented as fold change to the level expressed in control BEAS-2B cells.

Results

Metal concentration of PM samples

Jeddah, the second largest city in the Kingdom of Saudi Arabia, is bordered by the Red Sea in the west and the Al-Sarawat Mountains in the northeast, east and southeast. As in many other cities in the Arabian Peninsula, sand storms are common in Jeddah, and normally peak during the summer season. A total of 30 PM_{10} samples on Teflon filters were collected from the campus of King Abdulaziz University between June and September 2011, a time period that most faculty and students were on summer vacation. The PM_{10} that was captured in 3 air filters was collected during the sand storms (designated as the storm group), and PM_{10} captured in 27 other air filters represented the air particles for the typical summer vacation days (designated as the normal group). By using nondestructive XRF, we analyzed the concentration of 27 elements in PM_{10} (Table 1). Silicon concentration was the highest among 27 elements in both normal and storm samples, followed by calcium, sulfur, aluminum and iron (Table 1), which represented a typical source category of resuspended soil. Except for sulfur, the concentrations of silicon, calcium, aluminum and iron were increased in the storm samples, suggesting that the soil resuspension was the major source factor that accounted for the increased mass during the sand storm. In addition, the storm group exhibited a slight decrease in the concentration of most other metal elements, including those representing marine aerosol (sodium, chlorine), fuel combustion (nickel, vanadium, sulfur), mixed industrial (zinc, copper) and traffic sources (lead, bromine, selenium). Interestingly, several metal elements including cadmium, strontium, titanium and cobalt were increased in the storm group, probably originating from a local industrial source.

Gene expression profiles in BEAS-2B cells exposed to PM_{10}

To investigate the effects of PM in human lung cells, PMs collected in polypropylene filters were extracted and used to treat immortalized human bronchial epithelial BEAS-2B cells *in vitro*. One filter from each group was selected based on the metal concentration closest to the mean concentration. BEAS-2B cells were exposed to PM_{10} at various doses (0, 10, 25, 50, 100, and 200 $\mu g/cm^2$) for 1, 2, 7 and 14 days, and cytotoxicity was measured by cell

viability using colony formation assay. Surprisingly, cells exposed to PM_{10}, even at the highest dose, did not exhibit any significant cytotoxicity (data not shown). It is possible that collected PM_{10} represents the normal daily exposure in a non-occupational setting, which may not be sufficient to reduce cell survival at the tested doses and time durations. Since microarray analysis is capable of detecting subtle changes in gene expression that occur at lower doses than those that trigger a significant phenotypic alteration, we performed a whole transcripts analysis using Affymetrix Human Gene 1.0 ST Array. The median dose (50 μg/cm^2) of PM_{10} from the normal or storm group was chosen to treat BEAS-2B cells for either short-term (1 day) or longer-term (4 days) exposure. Two independent sets of untreated control cells and PM_{10} treated cells were harvested, and subjected to gene expression analysis.

To explore the global impact of PM_{10} exposure on gene expression, we first performed a principal component analysis (PCA) to visualize the profile of all genes without any filtering. As shown in Figure 1A, the samples treated with PM_{10} were clearly separated from untreated control samples, indicating a detectable difference in the gene expression pattern between control and PM_{10} treated samples. In contrast, samples from the normal (normal air pollution in the absence of sand storm) group clustered closely to those from the storm group, suggesting a similar effect on gene expression profiles. Interestingly, samples from 1-day exposure (D1) were clustered separately from the 4-day exposure (D4) group, suggesting the impact of exposure duration on gene expression profiles. Similar effects can be seen in hierarchical clustering analysis of genes changed more than 1.5 fold (Figure 1B). Fold change analysis (one-way ANOVA, alpha level only) identified 140 and 251 entities that changed more than 1.5 fold in D1 and D4, respectively, from either the normal group or the storm group versus the untreated control group. It is important to note that the changed entities in normal versus control were almost identical to those in storm versus control, both in D1 and D4 (Supplemental Material, Figure 1A & 1B), further supporting the conclusion that PM_{10} from the normal or the storm group induced similar gene changes in cells (Figure 1). Thus, a common gene list shared between both groups was used to analyze the networks and pathways changed by PM_{10} exposure.

Gene expression profiles in BEAS-2B cells exposed to PM_{10} for 1 day

After removing unannotated and repeated entities, there was a total of 125 genes that significantly changed more than 1.5 fold in cells exposed to PM_{10} for 1 day compared to untreated control cells ($p \leq 0.05$). Among these genes, 58 were up-regulated, and 67 were down-regulated. Table 2 shows the top 15 up-regulated genes and top 15 down-regulated genes. Several genes known to be involved in the cell response to oxidative stress were significantly up-regulated, including *HMOX1* (3.0), *SLC7A11* (2.53), *STC2* (2.01), *SRXN1* (2.0), *GCLM* (1.89), and *SQSTM1* (1.8). Interestingly, the genes related to TGF-β signaling, including ligand *BMP4* (−2.06), transcription factor *SMAD6* (−1.98), as well as targets *ID1* (−1.81) and *ID2* (−1.89), were all decreased. The full gene list containing 125 of changed genes is presented as Supplemental Material, Table 1.

To investigate the biological function of genes differentially modulated by PM_{10} exposure, the list of genes changed more than 1.5-fold was uploaded into the Ingenuity Pathway Analysis (IPA) tool. The top two biological function categories (ranked by p-value) are “cellular growth and proliferation” and “cell death”, suggesting that one of the early events in PM exposed cells is a change in cell growth property. Genes associated with top biological functions include *ID1-3*, *CDKN2B*, *CCND1*, etc.

Gene network analysis of these differentially expressed genes revealed 16 significant networks. Among these networks, “cellular compromise, drug metabolism, cell death” were the top related network with 21 focus molecules and significance score of 43 (the negative

log of p value) (Figure 2A). Other interesting networks are “gene expression, cellular function and maintenance, skeletal and muscular system development and function” (score: 34); “cell death, cellular development, hematological system development and function” (score: 23); “nutritional disease, cancer, organismal development” (score: 21); and “connective tissue disorders, inflammatory disease, cancer” (score: 21). The top five gene networks, along with their significance scores, number of genes involved, and names of differentially expressed genes, were listed as Supplemental material, Table 2.

In addition to the analysis of gene networks, we also analyzed the top canonical pathways associated with differentially expressed genes. Hepatic fibrosis pathway ($p= 1.46 \times 10^{-6}$) and NRF2-mediated oxidative stress response ($p= 8.8 \times 10^{-5}$) were the top two most represented canonical pathways (Figure 2C). Further analysis of genes associated with human diseases revealed that genes changed in 1-day exposure were linked to inflammation, connective tissue disorders and respiratory disease.

Other than biological function analysis, IPA also provided a useful tool, IPA-Tox, to identify the key functions and pathways that are changed upon treatment with toxic compounds and linked the changed gene expression profiles to clinical pathology endpoints. Interestingly, the top pathway identified in up-regulated genes was NRF2-mediated oxidative stress response ($p= 9.85 \times 10^{-6}$), which is consistent with the canonical pathway analysis. The top pathways identified in down-regulated genes were TGF-β signaling ($p= 0.0046$).

IPA’s newest transcription factor analysis represents a novel approach to predict the activation or inhibition of transcription factors based on the expression pattern of genes downstream of those factors. Although there is no significant change in mRNA level of *NFE2L2* gene (encoding NRF2 protein), NRF2 was identified as the most activated transcription factor (Z-score: 3.124) in PM exposed cells after 1-day exposure. Based on the expression levels of downstream targets, the second most active transcription factor predicted was AHR (Z-score: 2.54), which is known to be involved in drug metabolism and cell detoxification (Figure 2B).

Gene ontology analysis with genes changed more than 1.5-fold after PM exposure identified “response to oxidative stress” as the highly represented biological process in up-regulated genes, which further support the results obtained from IPA analysis (Supplemental Material, Table 3). Moreover, KEGG pathway analysis revealed “TGF-β signaling pathway” (p-value: 9.2×10^{-8}) was the most represented in down-regulated genes. A number of genes involved were down-regulated, including *BMP4*, *NOG*, *SMAD9*, *CDKN2B*, *SMAD6*, *ID1-3*.

Gene expression in BEAS-2B cells exposed to PM_{10} for 4 days

A total of 230 genes were significantly changed more than 1.5-fold in 4-day exposed cells compared to untreated control cells, including 147 up-regulated genes and 73 down-regulated genes. Table 3 showed the top 15 up- and down-regulated genes, and the complete list of genes changed more than 1.5-fold can be found in Supplemental Material, Table 4.

IPA analysis of differentially expressed genes revealed that the top two biological functions were “cellular movement” and “lipid metabolism”, suggesting a switch from an early response of cell growth or death to a later adaptive response including the changes involving mobility and metabolism. A total of 18 significant gene networks were associated with genes changed after a 4-day exposure. Among these networks, “lipid metabolism, small molecule biochemistry, vitamin and mineral metabolism” had the highest significant score (44) and 24 focus molecules (Figure 3A). Other interesting networks included “developmental disorder, hematological disease, immunological disease” (score: 42);

"behavior, cellular development, hematological system development and function" (score: 41); "cellular growth and proliferation, tumor morphology, cardiovascular system development and function" (score: 32); and "cell morphology, nervous system development and function, cell death" (score: 30). Supplemental Material, Table 5 lists the top five gene networks, along with their significance scores, number of genes involved, and the names of differentially expressed genes.

The top represented canonical pathway revealed by IPA analysis was "biosynthesis of steroids" ($p= 7.58 \times 10^{-6}$), followed by LXR/RXR activation ($p= 8.91 \times 10^{-4}$) and TR/RXR activation ($p= 9.94 \times 10^{-4}$) (Figure 3B). The top human diseases associated with these changed genes included cancer, gastrointestinal disease and metabolic disease. While cholesterol biosynthesis ($p= 1.28 \times 10^{-7}$) was identified as the top pathway in IPA-Tox in up-regulated genes, hepatic fibrosis ($p= 7.03 \times 10^{-5}$) was the top Tox pathway in down-regulated genes. The top Tox functions of the changed gene expression were hepatocellular carcinoma ($p= 4.08 \times 10^{-4}$), renal tubule injury ($p= 2.09 \times 10^{-4}$), and liver stenosis ($p= 0.00496$). Consistent with pathway analysis, SREBF1 and SREBF2, the genes encoding the master regulators of lipid and cholesterol synthesis, were found to be the most active transcription factors in the analysis. As seen in Figure 4, a number of genes downstream of either *SREBF1* or *SREBF2*, were up-regulated after 4 day PM_{10} exposure. Other active or inhibited transcription factors included *NR1I2*, *NR1H3*, *SMAD4*, *MTPN*, and *CTNNB1*.

Gene ontology analysis with differentially expressed genes confirmed the results of IPA analysis (Supplemental Material, Table 6). The top five represented biological processes in up-regulated genes were associated with sterol, cholesterol and lipid biosynthesis and metabolism. The KEGG pathway analysis revealed the steroid biosynthesis and PPAR signaling pathway as the top changed pathways in up-regulated genes after a 4-day exposure.

Effects of exposure duration on gene expression

Both IPA and Gene Ontological Analysis revealed distinct gene networks and pathways in D1 and D4 samples, suggesting an impact of exposure duration on gene expression changes and cellular responses. We then compared gene changes in D1 and D4 groups. As shown in Supplemental Material, Figure 1C, about 50% of the genes changed in D1, both up- and down-regulated, were also changed in D4. However, these commonly changed genes represented only 1/5 of up-regulated and 1/3 of down-regulated genes that were altered in D4. When the altered genes in both D1 and D4 were carefully examined, we found that more than 50% of gene expression correlated to the exposure duration. For example, *SERPINB2*, also known as Plasminogen activator inhibitor-2, increased about 3.9-fold at D1 but 10-fold in D4. *TNFRSF11B* is down-regulated about 1.8 fold after one day exposure but decreased about 5.6 fold after 4 day exposure. Thus, some genes exhibited exposure duration dependent expression changes.

Gene expression validation

To validate the gene expression changes observed in the microarray analysis, BEAS-2B cells were exposed to 50 $\mu g/cm^2$ of PM_{10} from the normal or the storm group for 1 or 4 days. Total RNA were extracted from two independent sample sets, and subjected for quantitative real time PCR of selected genes. Gene fold changes were compared to those obtained from microarrays. *HMOX1*, *IGFBP3*, *DDIT3* and *SLC7A11* were chosen as genes significantly changed after 1-day exposure. *SREBF1*, *SREBF2*, *HMGCS1*, *INAIG1*, *IDI1*, *CYP1B1* and *IGFBP3* were analyzed for the 4-day exposure. Table 4 summarizes the average fold change of these selected genes in microarray analysis, as well as the corresponding real-time PCR results.

Discussion

Numerous epidemiological studies have established an association between high concentration of PM and pulmonary cardiovascular disease. Studies using either cultured cells or animal models uncovered that a series of early events, including oxidative stress, inflammation and cytokine production, were likely the mediators of PM induced adverse health problems (Akhtar et al. 2011; Brook et al. 2010; Chen and Lippmann 2009; Rückerl et al. 2011). However, the cellular and molecular mechanisms underlying PM induced adverse health effects are largely unknown. Our results indicated that PM_{10} exposure of cultured cells resulted in significant changes in the global gene expression profile. In addition, exposure duration had an important impact on the type of gene expression changes. While a short-term exposure (1 day) modulated genes involved in cell response to oxidative stress and drug metabolism, a more extended exposure (4 days) resulted in expression changes in genes involved in inflammation, cytokine production, and cell metabolism. Strikingly, a number of SREBPs downstream target genes that were important for cholesterol and triglyceride biosynthesis were significantly upregulated after 4-day exposure, suggesting a possible link between PM_{10} exposure and the dysregulation of cholesterol and fatty acid metabolism.

One of the earliest events following PM_{10} exposure was a cell protective response to oxidative stress that was mainly caused by ROS production (Ghio et al. 2012; Araujo and Nel 2009; Møller et al. 2010). Studies have shown that ROS can be generated by transition metals in the PM via a Fenton reaction or by cellular detoxification enzymes (Cho et al. 2005; Becker et al. 2005). When the levels of ROS are high, cells initiate a protective response by stabilizing and activating the transcription factor NRF2 (Araujo and Nel 2009; Diabaté et al. 2011). Once it has been activated, NRF2 translocates into the nucleus and induces the transcription of more than 200 downstream targets genes including antioxidants and detoxification enzymes (Malhotra et al. 2010). IPA analysis of transcription factors revealed that NRF2 was the most active transcription factor in cells exposed to PM_{10} for 1-day (Figure 2). Many NRF2 target genes were up-regulated (Table 2), including antioxidant enzymes HMOX1 (3.03), NQO1 (1.72), TXRND1 (1.5), SRXN1 (2.0), enzyme involved in glutathione synthesis GCLM (1.89), and cysteine-glutamate transporter SLC7A11 (2.53), indicating PM_{10} exposure induced oxidative stress and initiated antioxidant defense in BEAS-2B cells. Our results from 1-day exposure are consistent with several recent studies on PM induced gene expression changes (Akhtar et al. 2010; Dergham et al. 2012; Diabaté et al. 2011; Gualtieri et al. 2012; Huang et al. 2009; Huang et al. 2011; Murphy et al. 2008; Riechelmann et al. 2007; Ross et al. 2007; Watterson et al. 2007).

AHR was predicted by IPA as the second most active upstream regulator in BEAS-2B cells exposed to PM for 1-day (Figure 2), which is supported by increased levels of its downstream targets including both phase 1 (CYP1B1, 1.45) and phase II (NQO1, 1.73) detoxification enzymes. With an extended 4-day exposure, the levels of CYP1B1 and NQO1 continued to increase reaching 3.12 and 2.35, respectively, suggesting a time dependent response of AHR activation. As a major receptor for polycyclic aromatic hydrocarbons (PAHs), AHR and its downstream targets play an important role in mediating cell adaptation and detoxification in response to environmental PAHs. PM induced AHR activation and subsequent induction of detoxification enzymes have been reported in A549, BEAS-2B and other cell types (Courter et al. 2008; Dieme et al. 2012; Gualtieri et al. 2011; Gualtieri et al. 2012; Mahadevan et al. 2005).

Another interesting finding was the up-regulation of genes related to cholesterol and lipid biosynthesis in cells exposed to PM_{10} for 4 days. Both IPA and Gene Ontology analysis indicated that lipid metabolism, particularly cholesterol and sterol biosynthesis, were the

most enriched gene network in cells exposed to PM_{10} for 4 days compared with untreated control cells. Consistent with functional analysis, pathways analysis revealed the biosynthesis of steroids as the most represented canonical pathway. Moreover, *SREBF1* and *SREBF2* genes were identified as the most active transcription factors in PM_{10} exposed cells based on the changes in their downstream target genes.

SREBF1 and *SREBF2* genes encode three basic helix-loop-helix (bHLH) lucine zipper proteins: SREBP1a, SREBP1c and SREBP2, which are master regulators of cholesterol and fatty acid biosynthesis (Eberlé et al. 2004; Shimano 2009; Ye and DeBose-Boyd 2011). SREBPs are synthesized in their precursor forms and stored in the endoplasmic reticulum (ER), which normally forms a complex with the SREBP-cleavage activating protein (SCAP) that can function as a sterol sensor (Bengoechea-Alonso and Ericsson 2007). In sterol-depleted cells, SCAP transports SREBPs from the ER to the Golgi, where the mature form of SREBPs are released by proteolytic cleavage and subsequently translocated to the nucleus to stimulate downstream target genes. While SREBP1a and 1c preferentially regulate genes involved in triglyceride and fatty acid synthesis, SREBP2 activates genes that control cholesterol and sterol biosynthesis (Bengoechea-Alonso and Ericsson 2007; Horton et al. 2003).

Multiple lines of evidence suggested an activation of both SREBP1 and SREBP2 in cells exposed to PM_{10} for 4 days. First, a large number of genes that participated in almost every step of the cholesterol synthesis pathway were up-regulated in PM_{10} exposed cells compared to untreated control cells (Figure 5). Although the fold enrichment ranged between 1.28 and 2.44, the finding was quite striking with the activation of almost the entire pathway controlled by SREBP2. Second, the mRNA levels of several important enzymes involved in synthesis of monosaturated fatty acids from acetyl-CoA were increased in PM_{10} exposed cells, such as acetyl-CoA carboxylase, fatty acid synthase, long-chain fatty acyl elongase, and steroyl-CoA desaturase, which are known targets of SREBP1c (Horton et al. 2003). Moreover, the mRNA levels of three enzymes (Malic enzyme 1, G6PD, and PGDH) that are activated by both SREBP1 and SREBP2 and required for generating NADPH from various sources were increased in PM treated cells. Last and most important, the mRNA levels of *SREBF1* and *SREBF2* were also induced by PM exposure (Table 6, Supplemental Material, Table 3). Taken together, BEAS-2B cells following 4 days of exposure to PM_{10} showed increased gene expression and enhanced transcriptional activity of SREBPs.

It is not clear how PM_{10} activated SREBPs in BEAS-2B cells. Similar to many other transcription factors, SREBPs can be regulated at two levels: transcriptional and posttranslational. One important transcriptional regulator of SREBPs is liver X-activated receptor (LXR) (Eberlé et al. 2004; Raghow et al. 2008). LXRs form heterodimers with retinoid X receptor and bind to SREBPs promoter to activate transcription, and thus play an important role in cholesterol and fatty acid metabolism. Recent studies reported a novel role of LXR in protecting the lung from injury by activating antioxidant enzymes and inhibiting inflammatory gene expression (Birrell et al. 2007; Gong et al. 2009). Interestingly, the IPA pathway analysis identified LXR activation as the second most represented canonical pathway in PM exposed BEAS-2B cells (Figure 4b), suggesting a potential role of LXR in transcriptional regulation of SREBPs in these cells. Posttranslational regulation of SREBPs involving two rounds of proteolytic cleavage occurred in the ER-Golgi. ER stress and activation of the unfolded protein response (UFP) have been associated with dysregulation of SREBPs activation and cholesterol homeostasis (Colgan et al. 2011). Recently, several studies reported that airborne PM induced ER stress and UFP in human lung cells (Watterson et al. 2009; Laing et al. 2010). Our studies also showed increased levels of mRNA for Hsp70, Hsp90, PPP1R15A and DDIT3, suggesting a possible response to ER stress in PM_{10} exposed cells, which might account for the activation of SREBPs. Lastly, as

the members of bHLH transcription factor family, the transcriptional activity of SREBPs can be modulated by a group of negative regulator, Ids (Moldes et al. 1999; Rahmouni and Sigmund 2008). Three members of Id proteins, Id1-3, were significantly downregulated in PM exposed BEAS-2B cells, which may have resulted in enhanced SREBPs transcriptional activity in these cells.

We do not know whether PM_{10} induced SREBPs activation could result in enhanced cholesterogenesis and lipogenesis, since we studied bronchial epithelial cells, while the liver is the site for much of the body's cholesterogenesis and lipogenesis. It is worth noting that SREBPs are normally expressed at a low level in lung cells that require lipogenesis to maintain surfactant. Deregulation of lipogenesis has been reported to cause lung damage (Plantier et al. 2012; Besnard et al. 2009). In addition, BEAS-2B cells may provide a better representation of the *in vivo* airway epithelial when they are cultured *in vitro* at the air-liquid interface. It is not clear whether the results from our study represented the changes of gene and pathway that occurred *in vivo*. Further profiling of gene expression changes and analyzing the cholesterol and triglyceride levels *in vivo* following long-term PM exposure will address these questions. In summary, our study is the first to report that PM_{10} exposure can modulate genes related to cholesterol and lipid metabolism, providing a new insight into the mechanisms underlying PM induced cardiovascular disease.

Supplementary Material

Refer to Web version on PubMed Central for supplementary material.

Acknowledgments

We would like to thank NYU Cancer Institute Genomics Facility for microarray hybridization and scanning. This work was funded by King Abdulaziz University (KAU), Jeddah, under grant number 4/00/00/252.

References

Akhtar US, Scott JA, Chu A, Evans GJ. In vivo and In vitro Assessment of Particulate Matter Toxicology. Urban Airborne Particulate Matter. 2011:427–449.

Akhtar US, McWhinney RD, Rastogi N, Abbatt JPD, Evans GJ, Scott JA. Cytotoxic and proinflammatory effects of ambient and source-related particulate matter (PM) in relation to the production of reactive oxygen species (ROS) and cytokine adsorption by particles. Inhal Toxicol. 2010; 22(Suppl 2):37–47. [PubMed: 21142797]

Araujo JA, Nel AE. Particulate matter and atherosclerosis: role of particle size, composition and oxidative stress. Part Fibre Toxicol. 2009; 6:24. [PubMed: 19761620]

Becker S, Dailey LA, Soukup JM, Grambow SC, Devlin RB, Huang YCT. Seasonal Variations in Air Pollution Particle-Induced Inflammatory Mediator Release and Oxidative Stress. Environ Health Perspect. 2005; 113:1032–1038. [PubMed: 16079075]

Bell ML, Davis DL. Reassessment of the lethal London fog of 1952: novel indicators of acute and chronic consequences of acute exposure to air pollution. Environ Health Perspect. 2001; 109(Suppl 3):389–394. [PubMed: 11427388]

Bengoechea-Alonso MT, Ericsson J. SREBP in signal transduction: cholesterol metabolism and beyond. Curr Opin Cell Biol. 2007; 19:215–222. [PubMed: 17303406]

Besnard V, Wert SE, Stahlman MT, Postle AD, Xu Y, Ikegami M, Whitsett JA. Deletion of Scap in alveolar type II cells influences lung lipid homeostasis and identifies a compensatory role for pulmonary lipofibroblasts. J Biol Chem. 2009; 284:4018–4030. [PubMed: 19074148]

Birrell MA, Catley MC, Hardaker E, Wong S, Willson TM, McCluskie K, Leonard T, Farrow SN, Collins JL, Haj-Yahia S, Belvisi MG. Novel role for the liver X nuclear receptor in the suppression of lung inflammatory responses. J Biol Chem. 2007; 282:31882–31890. [PubMed: 17766241]

Brook RD, Rajagopalan S, Pope CA, Brook JR, Bhatnagar A, Diez-Roux AV, Holguin F, Hong Y, Luepker RV, Mittleman MA, Peters A, Siscovick D, Smith SC, Whitsel L, Kaufman JD. American Heart Association Council on Epidemiology and Prevention, Council on the Kidney in Cardiovascular Disease, and Council on Nutrition, Physical Activity and Metabolism. . Particulate matter air pollution and cardiovascular disease: An update to the scientific statement from the American Heart Association. Circulation. 2010; 121:2331–2378. [PubMed: 20458016]

Chen LC, Lippmann M. Effects of metals within ambient air particulate matter (PM) on human health. Inhal Toxicol. 2009; 21:1–31. [PubMed: 18803063]

Cho AK, Sioutas C, Miguel AH, Kumagai Y, Schmitz DA, Singh M, Eiguren-Fernandez A, Froines JR. Redox activity of airborne particulate matter at different sites in the Los Angeles Basin. Environ Res. 2005; 99:40–47. [PubMed: 16053926]

Colgan SM, Hashimi AA, Austin RC. Endoplasmic reticulum stress and lipid dysregulation. Expert Rev Mol Med. 2011; 13:e4. [PubMed: 21288373]

Courter LA, Luch A, Musafia-Jeknic T, Arlt VM, Fischer K, Bildfell R, Pereira C, Phillips DH, Poirier MC, Baird WM. The influence of diesel exhaust on polycyclic aromatic hydrocarbon-induced DNA damage, gene expression, and tumor initiation in Sencar mice in vivo. Cancer Lett. 2008; 265:135–147. [PubMed: 18353537]

Dergham M, Lepers C, Verdin A, Billet S, Cazier F, Courcot D, Shirali P, Garçon G. Prooxidant and Proinflammatory Potency of Air Pollution Particulate Matter (PM(2.5-0.3)) Produced in Rural, Urban, or Industrial Surroundings in Human Bronchial Epithelial Cells (BEAS-2B). Chem Res Toxicol. 2012; 25:904–919. [PubMed: 22404339]

Diabaté S, Bergfeldt B, Plaumann D, Ubel C, Weiss C. Anti-oxidative and inflammatory responses induced by fly ash particles and carbon black in lung epithelial cells. Anal Bioanal Chem. 2011; 401:3197–3212. [PubMed: 21626191]

Dieme D, Cabral-Ndior M, Garçon G, Verdin A, Billet S, Cazier F, Courcot D, Diouf A, Shirali P. Relationship between physicochemical characterization and toxicity of fine particulate matter (PM2.5) collected in Dakar city (Senegal). Environ Res. 2012; 113:1–13. [PubMed: 22284916]

Dockery DW, Pope CA, Xu X, Spengler JD, Ware JH, Fay ME, Ferris BG, Speizer FE. An association between air pollution and mortality in six U.S. cities. N Engl J Med. 1993; 329:1753–1759. [PubMed: 8179653]

Duvall RM, Norris GA, Dailey LA, Burke JM, McGee JK, Gilmour MI, Gordon T, Devlin RB. Source apportionment of particulate matter in the U.S. and associations with lung inflammatory markers. Inhal Toxicol. 2008; 20:671–683. [PubMed: 18464055]

Eberlé D, Hegarty B, Bossard P, Ferré P, Foufelle F. SREBP transcription factors: master regulators of lipid homeostasis. Biochimie. 2004; 86:839–848. [PubMed: 15589694]

Ghio AJ, Carraway MS, Madden MC. Composition of air pollution particles and oxidative stress in cells, tissues, and living systems. J Toxicol Environ Health B Crit Rev. 2012; 15:1–21. [PubMed: 22202227]

Gong H, He J, Lee JH, Mallick E, Gao X, Li S, Homanics GE, Xie W. Activation of the liver X receptor prevents lipopolysaccharide-induced lung injury. J Biol Chem. 2009; 284:30113–30121. [PubMed: 19717840]

Gordon T. Linking health effects to PM components, size, and sources. Inhal Toxicol. 2007; 19(Suppl 1):3–6. [PubMed: 17886043]

Gualtieri M, Ovrevik J, Mollerup S, Asare N, Longhin E, Dahlman HJ, Camatini M, Holme JA. Airborne urban particles (Milan winter-PM2.5) cause mitotic arrest and cell death: Effects on DNA, mitochondria, AhR binding and spindle organization. Mutat Res. 2011; 713:18–31. [PubMed: 21645525]

Gualtieri M, Longhin E, Mattioli M, Mantecca P, Tinaglia V, Mangano E, Proverbio MC, Bestetti G, Camatini M, Battaglia C. Gene expression profiling of A549 cells exposed to Milan PM2.5. Toxicol Lett. 2012; 209:136–145. [PubMed: 22178795]

Horton JD, Shah NA, Warrington JA, Anderson NN, Park SW, Brown MS, Goldstein JL. Combined analysis of oligonucleotide microarray data from transgenic and knockout mice identifies direct SREBP target genes. Proceedings of the National Academy of Sciences. 2003; 100:12027–12032.

Huang YC, Karoly ED, Dailey LA, Schmitt MT, Silbajoris R, Graff DW, Devlin RB. Comparison of gene expression profiles induced by coarse, fine, and ultrafine particulate matter. J Toxicol Environ Health A. 2011; 74:296–312. [PubMed: 21240730]

Huang YC, Li Z, Carter JD, Soukup JM, Schwartz DA, Yang IV. Fine ambient particles induce oxidative stress and metal binding genes in human alveolar macrophages. Am J Respir Cell Mol Biol. 2009; 41:544–552. [PubMed: 19251948]

Laden F, Neas LM, Dockery DW, Schwartz J. Association of fine particulate matter from different sources with daily mortality in six U.S. cities. Environ Health Perspect. 2000; 108:941–947. [PubMed: 11049813]

Laing S, Wang G, Briazova T, Zhang C, Wang A, Zheng Z, Gow A, Chen AF, Rajagopalan S, Chen LC, Sun Q, Zhang K. Airborne particulate matter selectively activates endoplasmic reticulum stress response in the lung and liver tissues. Am J Physiol Cell Physiol. 2010; 299:C736–C749. [PubMed: 20554909]

Maciejczyk P, Chen LC. Effects of subchronic exposures to concentrated ambient particles (CAPs) in mice. VIII. Source-related daily variations in in vitro responses to CAPs. Inhal Toxicol. 2005; 17:243–253. [PubMed: 15804942]

Mahadevan B, Keshava C, Musafia-Jeknic T, Pecaj A, Weston A, Baird WM. Altered gene expression patterns in MCF-7 cells induced by the urban dust particulate complex mixture standard reference material 1649a. Cancer Res. 2005; 65:1251–1258. [PubMed: 15735009]

Malhotra D, Portales-Casamar E, Singh A, Srivastava S, Arenillas D, Happel C, Shyr C, Wakabayashi N, Kensler TW, Wasserman WW, Biswal S. Global mapping of binding sites for Nrf2 identifies novel targets in cell survival response through ChIP-Seq profiling and network analysis. Nucleic Acids Res. 2010; 38:5718–5734. [PubMed: 20460467]

Moldes M, Boizard M, Liepvre XL, Fève B, Dugail I, Pairault J. Functional antagonism between inhibitor of DNA binding (Id) and adipocyte determination and differentiation factor 1/sterol regulatory element-binding protein-1c (ADD1/SREBP-1c) trans-factors for the regulation of fatty acid synthase promoter in adipocytes. Biochem J. 1999; 344(Pt 3):873–880. [PubMed: 10585876]

Murphy G, Rouse RL, Polk WW, Henk WG, Barker SA, Boudreaux MJ, Floyd ZE, Penn AL. Combustion-derived hydrocarbons localize to lipid droplets in respiratory cells. Am J Respir Cell Mol Biol. 2008; 38:532–540. [PubMed: 18079490]

Møller P, Jacobsen NR, Folkmann JK, Danielsen PH, Mikkelsen L, Hemmingsen JG, Vesterdal LK, Forchhammer L, Wallin H, Loft S. Role of oxidative damage in toxicity of particulates. Free Radic Res. 2010; 44:1–46. [PubMed: 19886744]

Nouh MS. Is the desert lung syndrome (nonoccupational dust pneumoconiosis) a variant of pulmonary alveolar microlithiasis? Report of 4 cases with review of the literature. Respiration. 1989; 55:122–126. [PubMed: 2549601]

Plantier L, Besnard V, Xu Y, Ikegami M, Wert SE, Hunt AN, Postle AD, Whitsett JA. Activation of sterol-response element-binding proteins (SREBP) in alveolar type II cells enhances lipogenesis causing pulmonary lipotoxicity. J Biol Chem. 2012; 287:10099–10114. [PubMed: 22267724]

Pope CA. Respiratory disease associated with community air pollution and a steel mill, Utah Valley. Am J Public Health. 1989; 79:623–628. [PubMed: 2495741]

Raghow R, Yellaturu C, Deng X, Park EA, Elam MB. SREBPs: the crossroads of physiological and pathological lipid homeostasis. Trends Endocrinol Metab. 2008; 19:65–73. [PubMed: 18291668]

Rahmouni K, Sigmund CD. Id3, E47, and SREBP-1c: fat factors controlling adiponectin expression. Circ Res. 2008; 103:565–567. [PubMed: 18796641]

Riechelmann H, Deutschle T, Grabow A, Heinzow B, Butte W, Reiter R. Differential response of Mono Mac 6, BEAS-2B, and Jurkat cells to indoor dust. Environ Health Perspect. 2007; 115:1325–1332. [PubMed: 17805423]

Ross AJ, Dailey LA, Brighton LE, Devlin RB. Transcriptional profiling of mucociliary differentiation in human airway epithelial cells. Am J Respir Cell Mol Biol. 2007; 37:169–185. [PubMed: 17413031]

Rükerl R, Schneider A, Breitner S, Cyrys J, Peters A. Health effects of particulate air pollution: A review of epidemiological evidence. Inhal Toxicol. 2011; 23:555–592. [PubMed: 21864219]

Schwartz J, Marcus A. Mortality and air pollution in London: a time series analysis. Am J Epidemiol. 1990; 131:185–194. [PubMed: 2403468]

Schwarze PE, Ovrevik J, Låg M, Refsnes M, Nafstad P, Hetland RB, Dybing E. Particulate matter properties and health effects: consistency of epidemiological and toxicological studies. Hum Exp Toxicol. 2006; 25:559–579. [PubMed: 17165623]

Shimano H. SREBPs: physiology and pathophysiology of the SREBP family. FEBS J. 2009; 276:616–621. [PubMed: 19143830]

Simkhovich BZ, Kleinman MT, Kloner RA. Air pollution and cardiovascular injury epidemiology, toxicology, and mechanisms. J Am Coll Cardiol. 2008; 52:719–726. [PubMed: 18718418]

Waness A, El-Sameed YA, Mahboub B, Noshi M, Al-Jahdali H, Vats M, Mehta AC. Respiratory disorders in the Middle East: a review. Respirology. 2011; 16:755–766. [PubMed: 21564399]

Watterson TL, Hamilton B, Martin R, Coulombe RA. Urban particulate matter causes ER stress and the unfolded protein response in human lung cells. Toxicol Sci. 2009; 112:111–122. [PubMed: 19675143]

Watterson TL, Sorensen J, Martin R, Coulombe RA. Effects of PM2.5 collected from Cache Valley Utah on genes associated with the inflammatory response in human lung cells. J Toxicol Environ Health A. 2007; 70:1731–1744. [PubMed: 17885930]

Ye J, DeBose-Boyd RA. Regulation of cholesterol and fatty acid synthesis. Cold Spring Harb Perspect Biol. 2011; 3

Zanobetti A, Schwartz J. Particulate air pollution, progression, and survival after myocardial infarction. Environ Health Perspect. 2007; 115:769–775. [PubMed: 17520066]

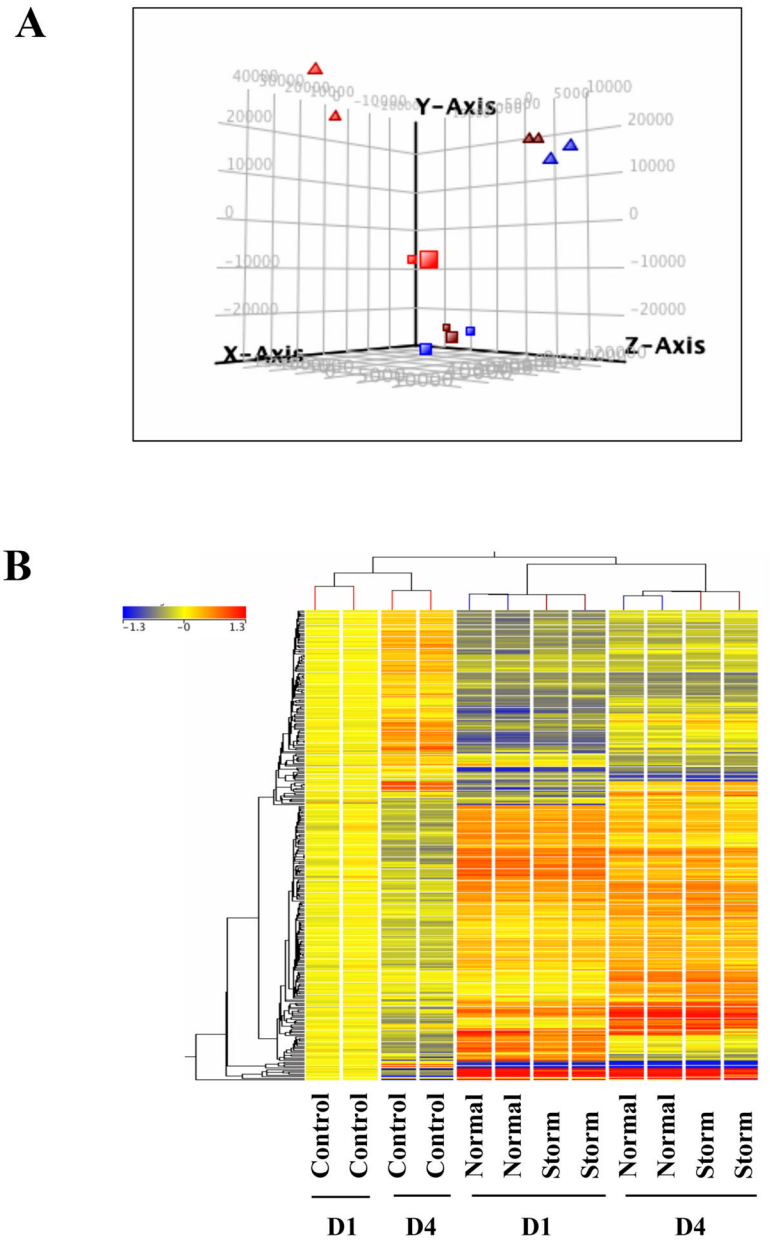

Figure 1.

Gene expression profiles of PM exposed cells. (**A**) Principal Components Analysis revealed distinct separation between control cells and PM exposed cells. Square: 1 day exposure; triangle: 4 day exposure; Red: control group; blue: normal group; brown: storm group. (B) Hierarchical cluster analysis of genes with more than 1.5-fold change in expression in one out of two groups (normal, storm) compared to untreated control cells. The bar relates the color code to the expression value determined after quantile normalization and baseline transformation to the median levels of control samples.

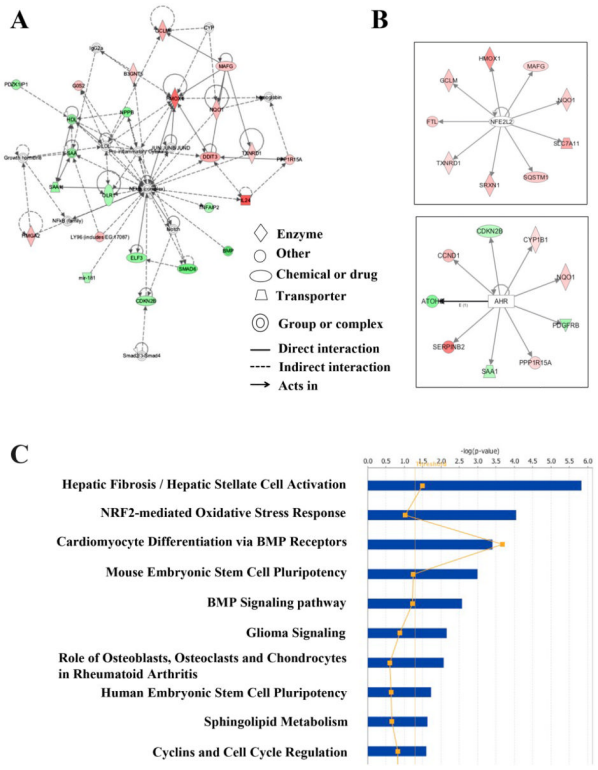

Figure 2.

Top gene networks and canonical pathways related with genes changed more than 1.5-fold after 1-day exposure. (**A**) Top represented gene network identified by Ingenuity Pathway Analysis (IPA). Color of each node indicates the regulation of gene expression. Red: up-regulation; green: down-regulation. (**B**) Most active transcription factors in genes changed more than 1.5-fold after 1-day exposure. The color of each downstream target of NRF2 or AHR indicated the regulation of gene expression. (**C**) Top 10 canonical pathways identified by IPA from genes changed more than 1.5-fold ($p \leq 0.05$). Bars represent −log (p-value) for significance; orange line represent the ratio of changed genes in the total number of genes in the specific pathway.

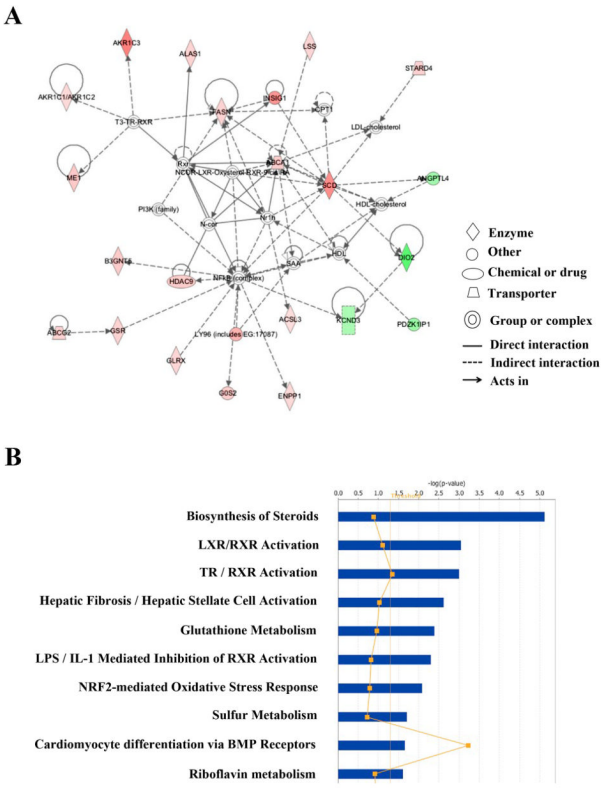

Figure 3.

Top gene networks and canonical pathways related with genes changed more than 1.5-fold after 4-day exposure. (**A**) Top represented gene network identified by Ingenuity Pathway Analysis (IPA). Color of each node indicates the regulation of gene expression. Red: up-regulation; Green: down-regulation. (**B**) Top 10 canonical pathways identified by IPA from genes changed more than 1.5-fold ($p \leq 0.05$). Bars represent −log (p-value) for significance; orange line represent the ratio of changed genes in the total number of genes in the specific pathway.

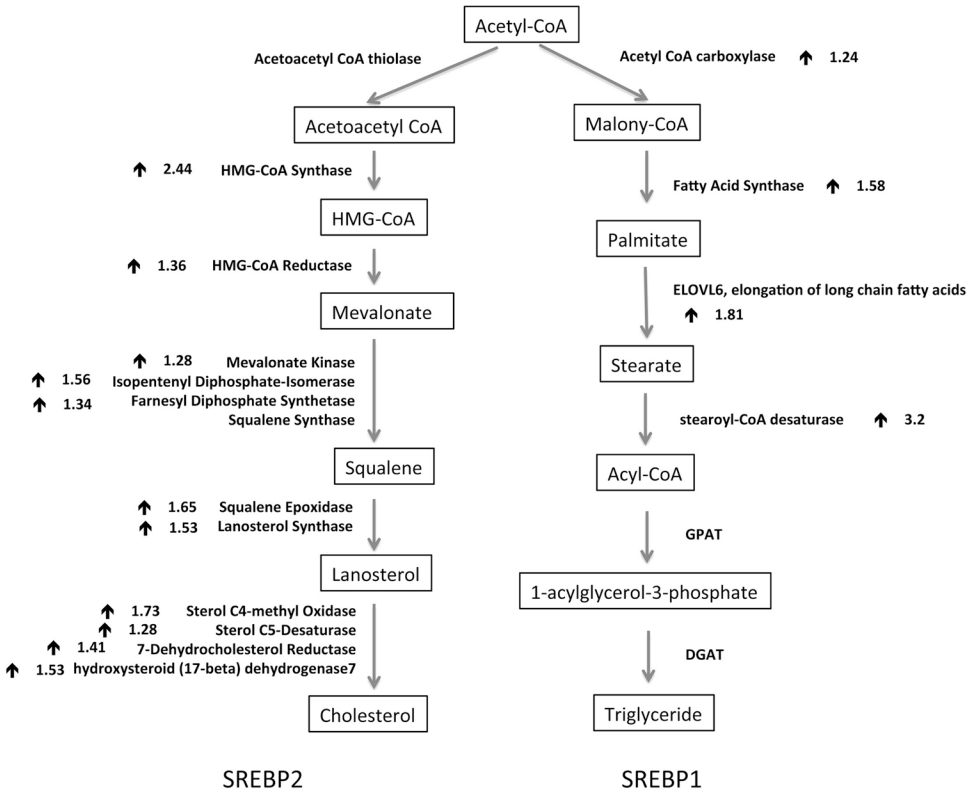

Figure 4.

Activation of genes involved in SREBPs mediated cholesterol and fatty acid synthesis in cells exposed to PM for 4 days. Downstream target genes of either SREBP2 (left) or SREBP1 (right) were listed in bold. The arrow (↑) indicated the up-regulation of mRNA levels, and number next to the arrow represented the average fold changes from duplicate microarray results.

Table 1

The concentrations of elements (ng/mg mass) in particles

	Normal		Storm	
Elements (ng/mg)	**Mean**	**S.D.**	**Mean**	**S.D.**
Sodium	**21335**	13621	**11425**	9351
Magnesium	**16465**	4167	**16050**	511
Aluminium	**35286**	11955	**41589**	16386
Silicon	**116194**	32378	**135499**	37820
Phosphorus	**1768**	714	**1884**	1018
Sulfur	**47620**	15311	**31932**	8777
Chlorine	**18722**	16545	**16487**	18881
Potassium	**8218**	2417	**7702**	946
Calcium	**55405**	17661	**67780**	35787
Titanium	**2819**	1013	**3781**	1851
Vanadium	**375**	132	**246**	53
Chromium	**95**	27	**109**	53
Manganese	**1079**	471	**1235**	63
Iron	**32152**	9934	**38044**	11484
Cobalt	**319**	119	**400**	133
Nickel	**132**	38	**100**	12
Copper	**243**	111	**141**	96
Zinc	**850**	823	**560**	124
Gallium	**54**	81	**29**	16
Germanium	**47**	86	**27**	45
Arsenic	**148**	228	**74**	101
Selenium	**47**	38	**38**	36
Bromine	**199**	78	**121**	63
Rubidium	**39**	23	**42**	9
Strontium	**304**	75	**476**	257
Cadmium	**1179**	1122	**1947**	2101
Lead	**3247**	6778	**943**	1408

Table 2

Top 15 up- and down-regulated genes ($p<0.05$) in day 1

Affymetrix Id	Genesymbol	Gene Name	Fold Changes	
			Normal	Storm
7951271	MMP1	matrix metallopeptidase 1	6.36	4.56
8021635	SERPINB2	serpin peptidase inhibitor, clade B, member 2	3.92	3.21
7909271	IL24	interleukin 24	3.50	3.43
8072678	HMOX1	heme oxygenase 1	3.03	2.23
8131844	GPNMB	glycoprotein nmb	2.81	2.83
8128123	RRAGD	Ras-related GTP binding D	2.68	2.69
8102800	SLC7A11	solute carrier family 7, member 11	2.53	1.65
8005475	TRIM16L	tripartite motif-containing 16-like	2.37	1.76
7942123	CCND1	cyclin D1	2.12	1.82
8084630	LOC344887	NmrA-like family domain containing 1 pseudogene	2.08	1.35
8115851	STC2	stanniocalcin 2	2.04	1.87
8092578	ETV5	ets variant 5	2.03	1.65
8064375	SRXN1	sulfiredoxin 1	2.00	1.55
8093104	TM4SF19	transmembrane 4 L six family member 19	1.97	1.90
7964460	DDIT3	DNA-damage-inducible transcript 3	1.94	1.88
8059279	EPHA4	EPH receptor A4	−1.81	−1.57
8152512	TNFRSF11B	tumor necrosis factor receptor superfamily, member 11b	−1.82	−2.09
8131666	ITGB8	integrin, beta 8	−1.83	−1.61
8115099	PDGFRB	platelet-derived growth factor receptor, beta polypeptide	−1.88	−1.71
7945232	ADAMTS15	ADAM metallopeptidase with thrombospondin type 1 motif, 15	−1.89	−1.66
8040103	ID2	inhibitor of DNA binding 2	−1.89	−1.65
7984353	SMAD6	SMAD family member 6	−1.98	−1.87
8092169	TNFSF10	tumor necrosis factor superfamily, member 10	−2.03	−1.65
7979241	BMP4	bone morphogenetic protein 4	−2.06	−1.71
7976567	BDKRB1	bradykinin receptor B1	−2.18	−2.17
8101429	PLAC8	placenta-specific 8	−2.18	−1.98
8043244	ATOH8	atonal homolog 8 (Drosophila)	−2.26	−1.90
8139488	IGFBP3	insulin-like growth factor binding protein 3	−2.27	−2.36
8146863	SULF1	sulfatase 1	−2.28	−2.19
7980485	DIO2	deiodinase, iodothyronine, type II	−4.19	−3.61

Table 3

Top 15 up- and down-regulated genes ($p<0.05$) in day 4

Affymetrix Id	Genesymbol	Gene Name	Fold Changes	
			Normal	Storm
7909271	IL24	interleukin 24	10.15	9.48
8021635	SERPINB2	serpin peptidase inhibitor, clade B, member 2	10.12	7.16
8131844	GPNMB	glycoprotein nmb	4.05	4.40
7925929	AKR1C3	aldo-keto reductase family 1, member C3	3.62	2.99
7929816	SCD	stearoyl-CoA desaturase (delta-9- desaturase)	3.20	3.71
8154381	C9orf150	chromosome 9 open reading frame 150	3.17	2.45
8051583	CYP1B1	cytochrome P450, family 1, subfamily B, polypeptide 1	3.12	3.37
8128123	RRAGD	Ras-related GTP binding D	3.10	3.19
8005475	TRIM16L	tripartite motif-containing 16-like	3.05	2.83
7951271	MMP1	matrix metallopeptidase 1	3.04	2.04
8137526	INSIG1	insulin induced gene 1	2.95	3.54
8152522	ENPP2	ectonucleotide pyrophosphatase/phosphodiesterase 2	2.83	2.62
8077899	PPARG	peroxisome proliferator-activated receptor gamma	2.79	2.45
8021301	RAB27B	RAB27B, member RAS oncogene family	2.55	2.88
8171435	PIR	pirin (iron-binding nuclear protein)	2.54	2.24
8083034	CLSTN2	calsyntenin 2	−1.86	−1.79
8102938	RNF150	ring finger protein 150	−1.89	−1.81
7916584	TACSTD2	tumor-associated calcium signal transducer 2	−1.89	−1.80
7909503	SERTAD4	SERTA domain containing 4	−1.94	−2.02
8095110	KIT	v-kit Hardy-Zuckerman 4 feline sarcoma viral oncogene homolog	−1.96	−1.80
8045664	LYPD6B	LY6/PLAUR domain containing 6B	−2.07	−2.13
8139488	IGFBP3	insulin-like growth factor binding protein 3	−2.11	−2.52
8069689	ADAMTS5	ADAM metallopeptidase with thrombospondin type 1 motif, 5	−2.14	−2.10
8058765	FN1	fibronectin 1	−2.15	−2.18
7980485	DIO2	deiodinase, iodothyronine, type II	−2.24	−2.97
7968417	FRY	furry homolog (Drosophila)	−2.26	−2.08
7912537	DHRS3	dehydrogenase/reductase member 3	−2.62	−2.60
7912520	NPPB	natriuretic peptide B	−2.91	−3.54
8146863	SULF1	sulfatase 1	−4.19	−3.89
8152512	TNFRSF11B	tumor necrosis factor receptor superfamily, member 11b	−5.59	−4.99

Table 4

Real-time PCR validation of microarray results

	Microarray		**qRT-PCR[a]**	
Day 1 (Fold change)	**Normal**	**Storm**	**Normal**	**Storm**
HMOX1	3.03	2.23	7.22	4.8
DDIT3	1.94	1.88	2.9	2.5
SLC7A11	2.53	1.65	2.45	1.69
IGFBP3	0.44	0.42	0.25	0.23
	Microarray		qRT-PCR[a]	
Day 4 (Fold change)	Normal	Storm	Normal	Storm
SREBF1	1.29	1.4	1.2	1.6
SREBF2	1.21	1.24	1.16	1.33
HMGCS1	2.44	2.59	3.1	3.9
INSIG1	2.92	3.54	3.9	5.6
IDl1	1.56	1.67	2.2	2.6
CYP1B1	3.12	3.37	5.7	5.6
IGFBP3	0.47	0.39	0.25	0.26

[a]The RT-PCR data represent the means of triplicates from two independent experiments, and are presented as fold change to the level expressed in control BEAS-2B cells.